

# DYNAMICS OF COULOMB-CORRELATED ELECTRON-HOLE PAIRS IN DISORDERED SEMICONDUCTOR NANOWIRES

I. VARGA<sup>1,2</sup>, C. SCHLICHENMAIER<sup>1</sup>, T. MEIER<sup>1</sup>, K. MASCHKE<sup>3</sup>,  
P. THOMAS<sup>1</sup> and S.W. KOCH<sup>1</sup>

<sup>1</sup>*Fachbereich Physik und Wissenschaftliches Zentrum für Materialwissenschaften, Philipps Universität, Marburg, D-35032 Marburg, Germany*

<sup>2</sup>*Elméleti Fizika Tanszék, Fizikai Intézet, Budapesti Műszaki és Gazdaságtudományi Egyetem, H-1521 Budapest, Hungary*

<sup>3</sup>*Institut de Physique Appliquée, École Polytechnique Fédérale de Lausanne, CH-1015 Lausanne, Switzerland*

The dynamics of optically generated electron-hole pairs is investigated in a disordered semiconductor nanowire. The particle pairs are generated by short laser pulses and their dynamics is followed using the Heisenberg equation of motion. It is shown that Coulomb-correlation acts against localization in the case of the two-interacting particles (TIP) problem. Furthermore, currents are generated using a coherent combination of full-gap and half-gap pulses. The subsequent application of a full-gap pulse after time  $\tau$  produces an intraband echo phenomenon  $2\tau$  time later. The echo current is shown to depend on the mass ratio between the electrons and the holes

## 1 Introduction

Optically generated carriers in a semiconductor environment produce an exciting scenario to study fast quantum coherent phenomena. The presence of disorder and the interaction between the carriers as well as with external fields produces a number of interesting phenomena<sup>1</sup>. The perspectives added by the recent fabrication of rings on a nanoscopic range<sup>2</sup> may add a further boost to the theoretical investigation of low-dimensional small semiconductor systems.

In this contribution we present two examples where the time evolution of the electron-hole pairs provides interesting insight into the combined effect of disorder and interaction. In the first one the spreading of initially localized electron-hole wave packets are shown to expand to considerably larger extent as compared to the size of single particle localization. In the second example we show how the phase coherent dynamics results in a new type of echo phenomenon discussed only recently.

## 2 The model and the equation of motion

The Hamiltonian of the two-band semiconductor subject to the external laser field represented by an electric field  $E(t)$  reads

$$H = \sum_{\lambda=e,h} H_{\lambda} + H_I + H_C, \quad (1)$$

where the two bands, the conduction band with electrons,  $H_e$ , and the valence band with holes,  $H_h$ , are both written in the tight-binding approximation

$$H_{\lambda} = \sum_i \varepsilon_i^{\lambda} \sigma_{ii}^{\lambda\lambda} - J^{\lambda} \sum_i (\sigma_{i,i+1}^{\lambda\lambda} + \sigma_{i,i-1}^{\lambda\lambda}). \quad (2)$$

The interaction with the laser is kept within the dipole approximation

$$H_I = -E(t)d, \quad \text{with} \quad d = -e \sum_{\lambda\lambda'i} (R_i \delta_{\lambda\lambda'} + r_{\lambda\lambda'}) \sigma_{ii}^{\lambda\lambda'} \quad (3)$$

and the Coulomb interaction within the monopole–monopole approximation

$$H_C = \frac{1}{2} \sum_{ij} (\sigma_{ii}^{ee} - \sigma_{ii}^{hh}) V_{ij} (\sigma_{jj}^{ee} - \sigma_{jj}^{hh}). \quad (4)$$

In the above equations we used  $\sigma_{ij}^{\lambda\lambda'} = a_{\lambda i}^\dagger a_{\lambda' j}$ , if  $a_{\lambda i}^\dagger$  ( $a_{\lambda i}$ ) creates (annihilates) a particle in the band  $\lambda$  ( $e$  or  $h$ ) at site  $i$ . Hence in Eq. (4) the electron densities are described using  $n_{ij}^e = \langle \sigma_{ij}^{ee} \rangle$  and the hole densities using  $n_{ij}^h = \delta_{ji} - \langle \sigma_{ji}^{hh} \rangle$ . The interband coherences (the pair amplitudes) are  $p_{ij} = \langle \sigma_{ij}^{eh} \rangle$ . The interaction between the carriers is assumed to have the regularized form of  $V_{ij} = V_0 a / (|i - j|a + a_0)$ , where  $a$  is the lattice constant,  $a_0$  and  $V_0$  characterize the strength of the interaction ensuring a finite value for the excitonic binding energy. For both of our studies they were fixed in order to obtain an exciton binding energy typical for quasi–onedimensional GaAs quantum wires.

In our study disorder entered by choosing the on–site energies  $\varepsilon_i^\lambda$  from a flat distribution of width  $W$ . These random values at each site for different bands may be anti-correlated if the energy separations of the isolated sites are constant and correlated if the averages of the site energies coincide.

The time evolution of the various components of  $\langle \sigma_{ij}^{\lambda\lambda'} \rangle$  are obtained via the solution of the Heisenberg equations of motion (using  $\hbar = 1$ )

$$i\partial_t \sigma_{ij}^{\lambda\lambda'} = [\sigma_{ij}^{\lambda\lambda'}, H] \quad (5)$$

In our first example we will simplify the equation assuming low excitation intensity. Thus linear response in the external laser field and henceforth the Hartree–Fock approximation for the particle–particle interaction are valid. This results for the interband coherences in

$$i\partial_t p_{ij} = (\epsilon_j^e + \epsilon_i^h - V_{ij}) - J^h (p_{i,j-1} + p_{i,j+1}) + J^e (p_{i-1,j} + p_{i+1,j}) - \mu_j E(t) \delta_{ij} \quad (6)$$

where  $\mu_j$  is the polarizability at site  $j$ . The intraband coherences, in this case, are calculated using the sum rules,  $n_{ij}^e = \sum_k p_{kj} p_{ki}^*$  and  $n_{ij}^h = \sum_k p_{jk} p_{ik}^*$  valid in this low excitation limit.

The second problem requires the external field to be handled nonperturbatively. Therefore as a first step we have omitted the particle–particle interaction or only kept it at the level similar to that presented in Eq. (6). In this case the term containing the external field would be  $eE(t) [(R_i - R_j)p_{ij} + r_{eh}(n_{ij}^e + n_{ji}^h - \delta_{ij})]$ . The intraband amplitudes,  $n_{ij}^e$  and  $n_{ij}^h$  are obtained in a similar fashion and have to be solved simultaneously.

### 3 Two interacting particles

The time evolution of an initially localized excitation has been followed via the integration of the equations of motion (6) for the interband coherences,  $p_{ij}$ . The extension of the wave packet  $p_{ij}$  was characterized, among others, by the center of mass width,  $R_{cm}^2 = \frac{1}{2} \sum_{ij} (i + j)^2 |p_{ij}|^2$ . A typical evolution of  $R_{cm}$  is given in Fig. 1. Here we used  $N = 240$  sites,  $J^e = -J^h = 20\text{meV}$  and very strong disorder,  $W^h = W^e = 4J^e$ .

The case of anti-correlated disorder seems to be much more favorable in order to produce reduced localization of the wave packets as is shown in Fig. 1. The numerically obtained time functions may be fitted with high accuracy to a phenomenological form of  $R(t) = ((Dt)^{-1/2} + \xi_\infty^{-1})^{-1}$  allowing a diffusion constant  $D$  and an extrapolated infinite time localization length  $\xi_\infty$  to be obtained from the fitting procedure<sup>4</sup>.

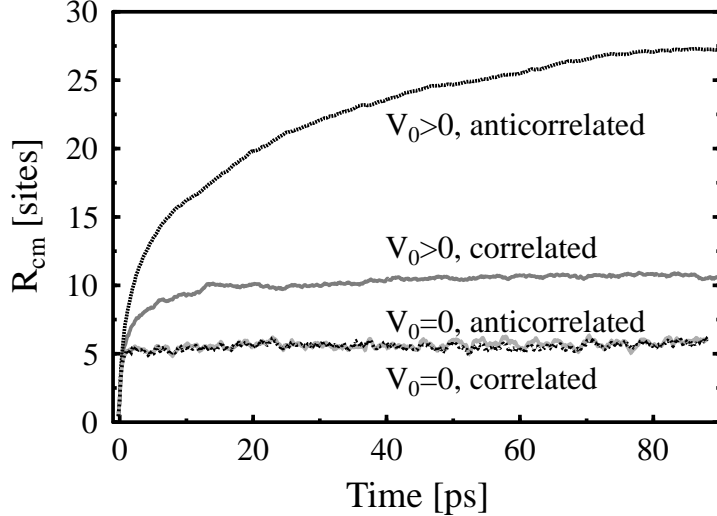


Figure 1: Center of mass width of a two-particle wave packet for correlated and anti-correlated disorder.  $J^e = -J^h = 20\text{meV}$ ,  $W^e = W^h = 4J^e$ . The curves have been obtained after averaging over 20 samples.

#### 4 Coherent control and current echo

In our other example we show how the rephasing process of *intra*band excitations after two subsequent laser pulses with a time delay of  $\tau$  can be investigated. This is in contrast to the photon echo which is similarly seen in the *inter*band excitation. The observable showing such an echo phenomenon is the total intra-band current.

The echo phenomenon has been first suggested using a voltage pump<sup>8</sup> for noninteracting particles. In the same scheme it has been shown that the many particle interaction reduces its height but does not destroy the current echo<sup>6</sup>. Recently the use of coherent control provides a further possibility to generate such an echo phenomenon<sup>7</sup>.

A current in the system (1)–(4) may be generated using a special excitation in which the initial populations are produced via transitions that have different initial propagation into different spatial directions, i.e. a spontaneous current appears. This scheme is an example of coherent control<sup>5</sup>. It is realized using a pulse with mean frequency in resonance with transitions in the optical continuum and another pulse having only half that frequency,  $E(t) = \text{Re} \{ E_1 e^{i\omega t + \phi_1} + E_2 e^{i\omega t/2 + \phi_2} \}$ . The resulting current can be calculated using the equation of motion,  $\mathcal{J} = \dot{d} = i[H, d]$  which results in a sum of two terms, an intra-band current,  $\langle \mathcal{J}_{intra} \rangle$ , and an inter-band current,  $\langle \mathcal{J}_{inter} \rangle$ . Here we give the former as  $\langle \mathcal{J}_{intra} \rangle \sim J^e \sum_i \text{Im}(n_{i+1,i}^e) - J^h \sum_i \text{Im}(n_{i+1,i}^h)$ .

The renewed excitation of the system with a laser pulse after time  $\tau$  causes phase conjugation. As it turns out we only need a light field with mean frequency  $\omega$  for the second excitation. This phase conjugation leads to a collective rephasing of the electron and the hole intra-band coherences,  $n_{ij}^{e,h}$ , at times<sup>9</sup>

$$T_e = \tau + \frac{J^h}{J^e} \tau \quad \text{and} \quad T_h = \tau + \frac{J^e}{J^h} \tau. \quad (7)$$

This is when the echo occurs in the conduction (valence) band for electrons (holes). Hence in the case when the holes are heavier than the electrons,  $J^e > J^h$ , the echo signal contains two peaks: one before  $t = 2\tau$  for the electrons and another one after that for the holes.

In Fig. 2 we give an example when the second excitation at  $t = 800\text{fs}$  has been simplified for a full gap pulse instead of the combination present at  $t = 0$ . That is the reason why we see only

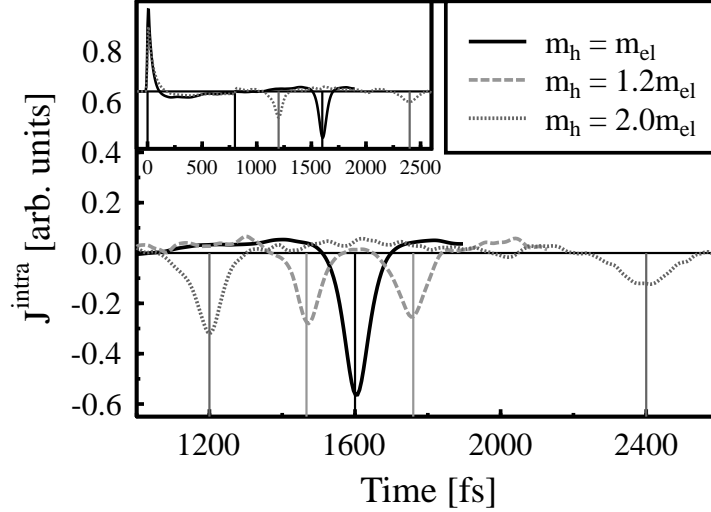


Figure 2: The echo time dependence on the effective mass of the particles. The inset shows the full time evolution with the first excitation at  $t = 0$ , the second excitation at  $t = 800$ fs using only a full gap pulse (producing a negligible response in the intraband current) and the spontaneous echo at  $t = 1600$ fs. In the main panel the variation of the echo peak is shown for various electron–hole mass ratios. The curves have been obtained as averages over 128 realizations of the disorder.

a minor change in the current response of the system at  $t = \tau$ . The double echo peak presented in Fig. 2 is obtained for a system consisting of  $N = 71$  sites, with  $m_e = 0.28m_0$ ,  $W^{e,h} = 2J^{e,h}$  and correlated disorder.

Note that the present model shows a photon echo even in the absence of disorder, while in that case there is no current echo. This emphasizes the fundamental difference of these two echo phenomena.

Work is in progress to study the influence of the many–particle interaction on this phenomenon in the coherent–control scenario.

## Acknowledgments

This work was supported by the Deutsche Forschungsgemeinschaft (DFG) through the Quantenkohärenz Schwerpunkt, by the Max-Planck Research prize, the Leibniz prize and the Hungarian Research Fund (OTKA) under T029813, T032116 and T034832.

## References

1. S. Weiser *et al.*, *Phys. Rev. B* **61**, 13088 (2000); C. Sieh *et al.* *Eur. Phys. J. B* **11**, 407 (1999); K. Maschke *et al.*, *Eur. Phys. J. B*, in press.
2. R.J. Warburton, *et al.* *Nature* **405**, 926 (2000).
3. D. Brinkmann, *et al.* *Eur. Phys. J. B* **10**, 145 (1999).
4. P. Thomas, *et al.* *phys. stat. sol. (b)* **218**, 125 (2000).
5. R. Atanasov, *et al.* *Phys. Rev. Lett.* **76**, 1703 (1996).
6. S. Sauter, *et al.* *Phys. Rev. B* **57**, 4299 (1998).
7. J. Stippler, *et al.* *phys. stat. sol. (b)* **221**, 379 (2000).
8. W. Niggenmeier, *et al.* *Phys. Rev. Lett.* **71**, 770 (1994).
9. C. Schlichenmaier, *Diploma Thesis* (Marburg, 2001), unpublished.